Soft Matter

ROYAL SOCIETY OF CHEMISTRY

PAPER

View Article Online
View Journal | View Issue

Cite this: *Soft Matter*, 2023, **19**, 3675

Surface properties influence marine biofilm rheology, with implications for ship drag†

Alexandra A. Snowdon, *[a] Simon P. Dennington,[a] Jennifer E. Longyear,[b] Julian A. Wharton [a] and Paul Stoodley [acd]

Marine biofilms on ship hulls increase frictional drag, which has economic and environmental consequences. It is hypothesised that biofilm mechanics, such as viscoelasticity, play a critical role in biofilm-associated drag, yet is a poorly studied area. The current study aimed to rheologically characterise ship-relevant marine biofilms. To combat marine biofilms on ship hulls, fouling-control coatings are often applied; therefore, the effect of different surfaces on marine biofilm mechanics was also investigated. Three surfaces were tested: a non-biocidal, chemically inert foul-release coating (FRC), an inert primer (ACP) and inert PVC. Physical properties of biofilms were explored using Optical Coherence Tomography (OCT) and a parallel-plate rheometer was used for rheological testing. Image analysis revealed differences in the thickness, roughness, and percent coverage between the different biofilms. Rheological testing showed that marine biofilms, grown on FRC and ACP acted as viscoelastic materials, although there were differences. FRC biofilms had a lower shear modulus, a higher viscosity, and a higher yield stress than the ACP biofilms, suggesting that the FRC biofilms were more readily deformable but potentially more robust. The results confirmed that surface treatment influences the structural and mechanical properties of ship-relevant marine biofilms, which could have implications for drag. A better understanding of how different surface treatments affect marine biofilm rheology is required to improve our knowledge on biofilm fluid–structure interactions and to better inform the coating industry of strategies to control biofilm formation and reduce drag.

Received 16th December 2022,
Accepted 28th April 2023

DOI: 10.1039/d2sm01647h

rsc.li/soft-matter-journal

1. Introduction

Marine biofilms are multi-cellular communities composed of micro-algal and bacterial components encased within a protective and hydrated matrix. The matrix is mainly composed of extracellular polymeric substances (EPS) that the organisms exude, which aids in attachment of a biofilm to a surface.[1,2] The EPS can be considered as a crosslinked polymer gel,[3–5] and is arranged with a system of pores and channels that contribute to the elastic and viscous behaviour of a biofilm.[6] Biofilms are viscoelastic entities, which exhibit a time dependent response when exposed to mechanical stress or strain that demonstrates both elastic and viscous elements. This behaviour has been reported as partly responsible for the recalcitrance of biofilms to external challenges, such as mechanical, chemical and medical,[7,8] since although biofilms are typically soft and deformable materials, they can dissipate imposed stresses through viscoelastic responses.[9–11] For example, biofilms have been shown to 'flow' in the form of ripple-structures when exposed to increased shear enabling parts of the biofilm to resist detachment from a surface[12,13] demonstrating that the viscoelastic nature of a biofilm has a role to play in biofilm survival.[8,14]

Marine biofilms induce significant economic and environmental consequences within the shipping industry[15] and can induce a 1–18% penalty in ship shaft power.[16,17] It is widely accepted that biofilms increase surface roughness of a ship hull which consequently increases biofilm-associated drag.[18,19] Yet, it has also been hypothesised that biofilm viscoelasticity increases drag too by dissipating energy through viscoelastic motion as well as disrupting the boundary layer by means such as streamer oscillation.[20,21] A deeper understanding of how marine biofilm physico-mechanical properties interact with one another and how these complex systems respond to external forces is required. To do this an important step is to characterize and quantify the elasticity and viscosity of marine biofilms.

[a] *National Centre for Advanced Tribology, Faculty of Engineering and Physical Sciences, Southampton University, UK. E-mail: a.Jackson@soton.ac.uk, s.p.dennington@soton.ac.uk, j.a.wharton@soton.ac.uk*
[b] *AkzoNobel/International Paint Ltd, Stoneygate Lane, Gateshead, UK. E-mail: jennifer.longyear@akzonobel.com*
[c] *National Biofilm Innovations Centre, School of Biological Sciences, Southampton University, UK*
[d] *Department of Microbial Infection and Immunity, The Ohio State University, Columbus, OH, USA. E-mail: paul.stoodley@osumc.edu*

† Electronic supplementary information (ESI) available. See DOI: https://doi.org/10.1039/d2sm01647h

The elasticity of medical and dental biofilms is reasonably well documented, ranging between a few Pa and several kPa.[22,23] In part, the large range is understandable given biofilm heterogeneity which makes it difficult to apply standard test methods.[24] It could be expected that marine biofilms would have a similar elasticity range, although it is important to note that the biological composition of a marine biofilm can differ considerably from medical or wastewater biofilms. Marine biofilms incorporate not only bacteria, but diatoms and microalgae, which add to their structural and EPS chemical complexity. Winston *et al.*, studied pond water biofilms with a micro-algal presence and found that they possessed a significantly lower shear modulus than that for bacterial biofilms.[25] More recently, Souza-Egipsy *et al.*, studied prokaryotic and eukaryotic biofilms from two sampling locations in acidic stream and found significant differences between the structural and mechanical properties.[11]

To combat biofilm formation and macrofouling on ship hulls fouling-control coatings are often applied. Traditionally, fouling-control coatings have routinely employed toxic biocides, which deter the settlement and growth of biofouling organisms.[26] Although often highly effective, such biocidal coatings release biocides and concerns about the potential harmful impact on the aquatic environment mean that the use of this type of coating is increasingly regulated on a national and international basis.[27] Therefore, the industry is moving towards non-biocidal alternatives, such as foul-release coatings (FRCs).[26] In simple terms, FRCs act as 'non-stick' elastomeric surfaces due to a low surface energy which makes it challenging for marine fouling organisms (such as diatoms) to bond to a surface and are substantially chemically inert.[28,29] Importantly, due to differences in the chemical composition, wettability, and surface roughness of different coatings different biological communities thrive on different coated surfaces.[2,30,31] In turn, a different microbial community could constitute a change in structural[32,33] and mechanical properties due to changes in EPS composition, concentration of bacterial cells and cohesiveness *etc.*,[11] which would consequently impact drag.[34] Therefore, to better understand how surface coatings alter the mechanical properties of a biofilm, rheological characterisation of marine biofilms grown on different surfaces was investigated.

The aims of our study were, firstly, to determine the structural and mechanical properties of marine biofilms, using OCT and a rotational parallel-plate rheometer. A rotational rheometer is perhaps the most cited equipment used for rheological characterisation of biofilms[35] as it can capture complex viscoelastic behaviour.[7,36,37] Modern rheometers allow both dynamic measurements in shear as well as axial indentation. Also, a rheometer offers high throughput experiments due to small test pieces and ease of application.[38] Furthermore, Optical Coherence Tomography (OCT) is a non-invasive method for visualising biofilms at the *meso*-scale and was employed to characterise the structural properties of the biofilms before and after rheological testing. The second aim was to compare the structural and mechanical profiles of biofilms grown on different surfaces.

2. Methodology

2.1. Coupons and surface treatments

Circular PVC coupons with a 40 mm diameter and 1 mm thickness (Chemical Process Solutions Ltd) were abraded with P80-grade sandpaper to promote the adhesion of paint to the coupon surface.

The paints used were commercial coatings provided by AkzoNobel:

- Intershield® 300 (ACP, n = 10) – a grey universal primer with long-term anti-corrosive properties and no anti-fouling properties (ACP).
- Intersleek® 1100SR (FRC, n = 10) – a grey non-biocidal, advanced fluoropolymer foul-release coating.

The paints were prepared according to manufacturer instructions (AkzoNobel) and a synthetic paint brush was used to ensure a surface with comparable roughness to untreated PVC, as confirmed using blue light interferometry (Fig. S1, ESI†). The ACP coupons were single coated whereas the FRC coupons followed a scheme of first an anticorrosive primer (ACP), then silicone tie-coat and finally the FRC top-coat was applied. Inert grey PVC coupons (PVC, n = 10) that had been abraded with P80-grade paper were used as a control surface for the rheometer experiments. It was important to keep surface colour consistent across all coupons to eliminate the potential impact of colour on the rheological properties of biofilms[39,40] (Fig. 1). For each surface type, ten coupons were prepared for fouling (total = 30 coupons).

2.2. Exposure to marine fouling

The coupons were attached to 15 cm × 10 cm glass plates (Fig. 1) using double-sided tape. Five identical coupons were attached to each glass plate (Fig. 1) and were immersed in a shallow indoor flow-through tank of natural seawater at Newcastle University's Dove Marine Laboratory (Cullercoats Bay, UK) under static conditions, so that no downstream effects of one coupon position influencing another was expected. The glass plates were immersed horizontally (in random positions) at the same depth to avoid differences in the biofilms driven differences in light availability caused by water depth. The seawater was filtered of larger particles and marine organisms and was lit naturally by a skylight window situated above the

Fig. 1 Coupons (40 mm dia.) attached to a glass plate before being immersed in a natural seawater tank at the Dove Laboratory (Cullercoats Bay, UK). From left to right there are FRC coupons, ACP and uncoated, sanded PVC coupons (control).

tank. The coupons were deployed on 24th February 2022 and were removed on 19th April 2022. Over this period, the seawater temperature was 7 to 10 °C. The coupons were removed carefully from the tank to avoid disruption to the biofilm structure and were transported to AkzoNobel (Felling, UK) for testing on a rheometer. Biofilms were kept hydrated during transportation by misting them with water taken from the Dove Laboratory tank.

Although marine biofilms in a real-world scenario are typically exposed to flow conditions, those tested here were cultivated under static conditions. This enabled the focus of the study to be on assessing the relationship between structural and mechanical properties of marine biofilms. Further, marine ships experience idle periods and are typically more vulnerable to biofilms and other fouling organisms during this time;[41] as biofilms are typically the first colonisers of a ship hull it would be useful to rheologically characterise them under both static and dynamic conditions.

2.3. Structural characterisation of biofilms using OCT

Before rheological testing the coupons covered with biofilm were characterised using OCT (Ganymede, ThorLabs). An OCT is a non-invasive, high throughput method for visualising and quantifying biofilm properties *in situ* at the *meso*-scale.[42] Briefly, an OCT is comprised of a light source (a superluminescent diode with a central wavelength of 930 nm was used in the present study) which penetrates the biofilm sample and creates a point reflection signal. The signal is then transformed into a depth-resolved intensity profile at one location to create an A-scan in the z-direction (height). A series of A-scans produces a cross-sectional image in the xz-plane (length-height), otherwise known as a B-scan (two-dimensional image). By acquiring consecutive B-scans along the y-axis (width) a volumetric representation of the sample is created and is called a C-scan (three-dimensional image).

In the present study, each coupon was immersed in a shallow dish filled with seawater taken from the tank at the Dove Laboratory and was then placed under the OCT. Three B-scans measuring 9.0 × 2.1 mm (xz) and a single C-scan measuring 9.0 × 9.0 × 2.1 mm (x, y, z) were taken of each coupon. The A-scan averaging was set to three to remove noise from the images and the OCT scan rate was 30 kHz. ThorLabs software, version 5.8.3 (Ganymede, ThorLabs), was used to control the OCT light, focus and imaging.

To quantify biofilm structural properties the C-scans were exported as.oct files from ThorLabs into MATLAB (version 2021B)[43] and were processed using custom MATLAB scripts produced by Fabbri *et al.*[44] For all coupons covered with biofilms, mean biofilm thickness (mm), percent coverage (%) and a roughness coefficient $\left(R_a^*\right)$ was calculated.[44,45] For more details on calculations please refer to the ESI.†

OCT analysis was conducted before and after rheological testing to assess the effect of stress on the structural characteristics of the biofilms. This also allowed a comparison between biofilms grown on different surfaces that had been exposed to comparative rheological testing procedures.

2.4. Rheometer

A Discovery Hybrid rheometer (HR10) (TA Instruments) was used to rheologically characterise the marine biofilms. The rheometer has a gap position resolution of 0.02 μm and a torque resolution of 1.0×10^{-10}. A parallel-plate set-up was adopted with a 40 mm stainless-steel sandblasted top-plate (TA Instruments) to create roughness for grip and to avoid slippage. All measurements were performed at 10 °C using a Peltier-plate heat exchanger (Fig. 2). It was important to test the biofilms at the temperature they had been cultivated at to avoid thermal shock. The biofilms were kept hydrated during testing by immersing them in a well filled with 4 mL of the seawater taken from the tank they were cultivated in.

Biofilms typically exhibit structural heterogeneity which could be expected to cause variability in rheometer measurements. Hence, we report the values for the whole biofilms (cells, EPS, trapped debris and water channels within the structure). In the open literature it has been suggested that controlling the gap thickness between the parallel plates using a constant normal force as opposed to biofilm thickness ensures sufficient contact between the biofilm and the rheometer top-plate, regardless of original heterogeneity, as evidenced by non-slippage using this strategy.[46] In this study, biofilms were compressed to a normal force of 0.1 N (±0.01 N) before testing. For each rheometer experiment three biological replicates were prepared. As rheometer tests can disrupt the mechanical integrity of a biofilm each replicate was tested once.

2.4.1 Amplitude sweeps. Amplitude sweeps were performed by incrementing oscillatory strain from 10^{-5} to 10^{-1} at an oscillation frequency of 1 Hz. The linear viscoelastic region (LVR) for the biofilms was determined from stress–strain curves where the stress was linear as a function of strain with an R^2 value >0.95. The yield stress (σ_y) was taken as the intersect of the storage (G') and loss moduli (G'').

2.4.2 Frequency sweeps. Frequency sweeps were executed by incrementing the oscillatory frequency from 0.1 to 10 Hz at a constant strain of 2.5×10^{-4} which was determined as being in the LVR for the biofilms grown on all coupons.

2.4.3 Creep-recovery. Creep-recovery tests were performed at different shear stress values: 0.25, 0.5, 0.75, 1.0, 1.25, 1.5, 1.75, 2.0, 5.0, 10 and 20 Pa. A constant stress was applied for 60 s at which point the stress was removed (0 Pa); recovery of

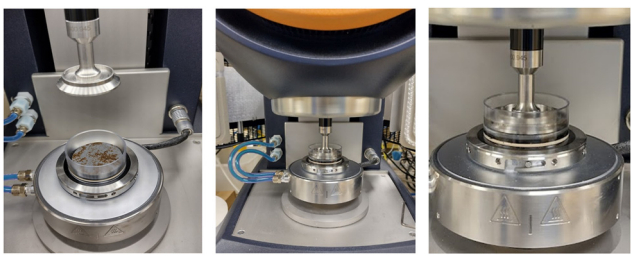

Fig. 2 The parallel-plate rheometer was set up with a Peltier plate and clear PVC well which was filled with seawater for testing.

the biofilm was then followed for 60 s. Strain was plotted as a function of time and effective shear modulus (G) and effective viscosity (η) were quantified.[47] η was calculated during the creep portion of the experiment:

$$\eta = \frac{\sigma}{\text{slope}} \quad (1)$$

where, σ is shear stress (Pa) and slope is the slope of the linear viscous region of the creep curve. The linear viscous region typically occurs towards the end of the creep portion of the experiment and can be taken as the area where the slope has reached $R^2 > 0.95$ (Fig. S2b, ESI†). From the recovery part of the experiment G was calculated using:

$$G = \frac{\sigma}{\Delta_\gamma} \quad (2)$$

where, Δ_γ is the elastic recovery which can be defined as the initial vertical drop in strain (Υ) that occurs when applied shear stress is removed (Fig. S2c, ESI†).

The elastic relaxation time (λ), which is the time it takes for a transition from elastic to viscous dominated behaviour when a biofilm is exposed to a constant stress, was calculated using:[48]

$$\lambda = \frac{\eta}{G} \quad (3)$$

2.5. Statistical analysis

Statistical analysis was executed in R Studio (version 1.1.423, R version 4.2.1)[49] and a P-value of <0.05 was deemed significant for all statistical outcomes.

To study the effect of rheological testing on the roughness coefficient $\left(R_a^*\right)$, mean thickness (mm) and percent coverage (%) of biofilms grown on each surface a Welch's two sample T-test was executed. A one-way ANOVA and a *post hoc* Tukey test was used to determine significant differences in the mechanical characteristics, namely G, η and λ, of biofilms grown on different surfaces. A Kruskal–Wallis and *post hoc* Dunn test was used as the non-parametric alternative if data did not fit the assumptions of an ANOVA. To measure differences between the physical characteristics of biofilms grown on different surfaces a Kruskal–Wallis was required.

3. Results

3.1. Characteristics of biofilms grown on different coupons

To test the hypothesis that ship-relevant marine biofilms grown on different coupons would display a variety of structural properties the biofilm characteristics were captured using an OCT. The effect of shear was also tested by using OCT before and after testing on the rheometer. Qualitatively, the biofilms grown on the FRC coupons (''FRC biofilms'') were thin with sparse small clumps in comparison to the 'fluffy' and thick biofilms covering the surface of the PVC and ACP coupons (''PVC biofilms'' and ''ACP biofilms'', respectively), see Fig. 3. Overall, all biofilms were brown in colour which signified a high diatom presence, confirmed by microscopy. Note that although three biological replicates were prepared for each rheometer test, some were discarded due to disturbances during transfer from the growth tank to the rheometer. Also, as there is no standard method of testing for rheologically characterising marine biofilms,[24,38] some coupons had to be utilised for method optimisation. As a consequence of

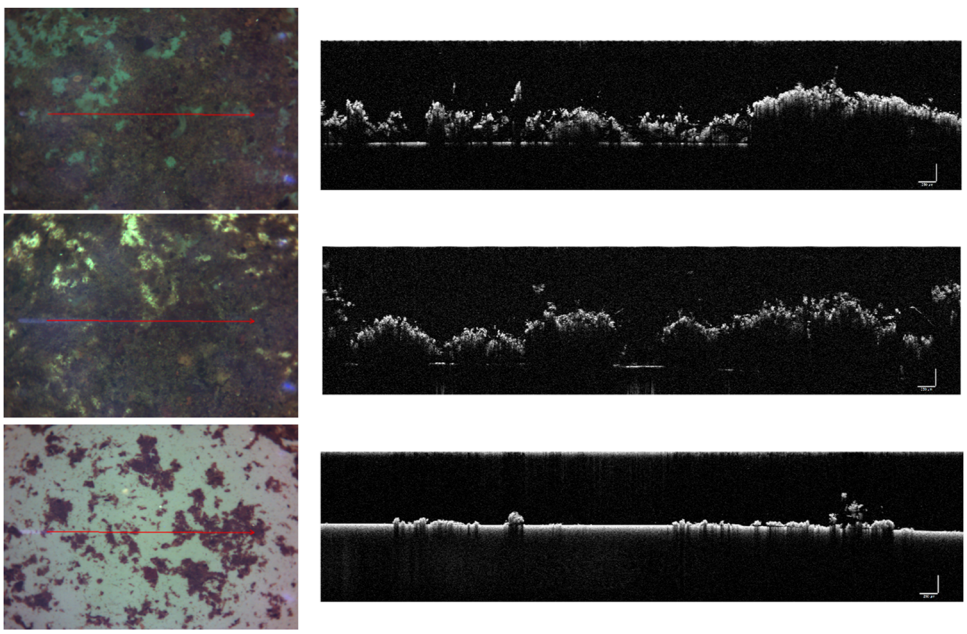

Fig. 3 Optical microscopy (left) and cross-sectional OCT two-dimensional (2D) scans (right) taken using an OCT, of the biofilms grown on different surfaces: top = PVC, middle = ACP, bottom = FRC. The red line in the photographs shows the direction of the 2D-scan on the right. The scale bar in the 2D-scans represents 250 μm.

fewer biological replicates, it was not possible to execute uncertainty analysis on all mechanical tests conducted.

Physical differences were confirmed by statistical analysis as shown in Fig. 4. Significant differences were found between the thickness (before testing) of the biofilms grown on the three coupon types (Kruskal–Wallis, $P < 0.05$) (Fig. 3 and 4b). The ACP biofilms had a significantly higher pre-testing R_a^* and a significantly lower pre-testing coverage than the PVC biofilms. Between ACP: FRC and PVC: FRC there were no significant differences in percent coverage and R_a^* (Kruskal–Wallis, $P > 0.05$). Across all variables, the biofilms grown on FRC coupons showed the lowest change when comparing structural properties pre- and post-testing, which suggests that the FRC biofilms are robust under testing conditions. For the ACP and PVC biofilms there was a significant difference between thickness before and after testing (Welch's two sample T-test, $P < 0.05$) (Fig. 4b), which could be linked to the removal of 'fluffy' surface layers when exposed to shear stress.

3.2. Rheological characterisation of marine biofilms

3.2.1 Amplitude sweeps. Oscillatory strain sweeps were performed by incrementally increasing strain (−) from 10^{-5} to 10^{1} at a controlled frequency of 1 Hz. The storage modulus (G', Pa), loss modulus (G'', Pa) and stress (σ, Pa) were calculated, and displayed in Fig. 5. The LVR was taken as the section where the stress–strain slope had an $R^2 > 0.95$; for all coupon types the LVR was comparable with respect to length and strain range (Fig. S3, ESI†).

The intersect of G' and G'' was taken as the yield stress, which indicates a shift from an elastic-response to a viscous-dominated response. The FRC biofilms displayed the greatest yield stress of 15 ± 4 Pa (n = 2), compared to 13 Pa (n = 1), for ACP biofilms and 11 Pa (n = 1), for the PVC biofilms, which suggests that the FRC biofilms were stronger than the others. The shape of the G' and G'' curves of PVC and ACP biofilms were comparable; after the LVR both showed a steady decline in G' and G'' with an increase in strain which continued past the yield stress point (shear thinning behaviour) (Fig. 5). Shear thinning behaviour is often reported for biofilms once the yield stress is reached[11,50] as it is indicative of disruption within the structure (such as slippage between polymer strands[51]) which could be expected as the biofilm is transitioning towards a more viscous-like response. Alternatively, for FRC biofilms, after the LVR, G''declined but G'' showed a slight increase until the yield stress was reached. This behaviour is often described as a weak strain overshoot[11,52] which occurs when there is a local

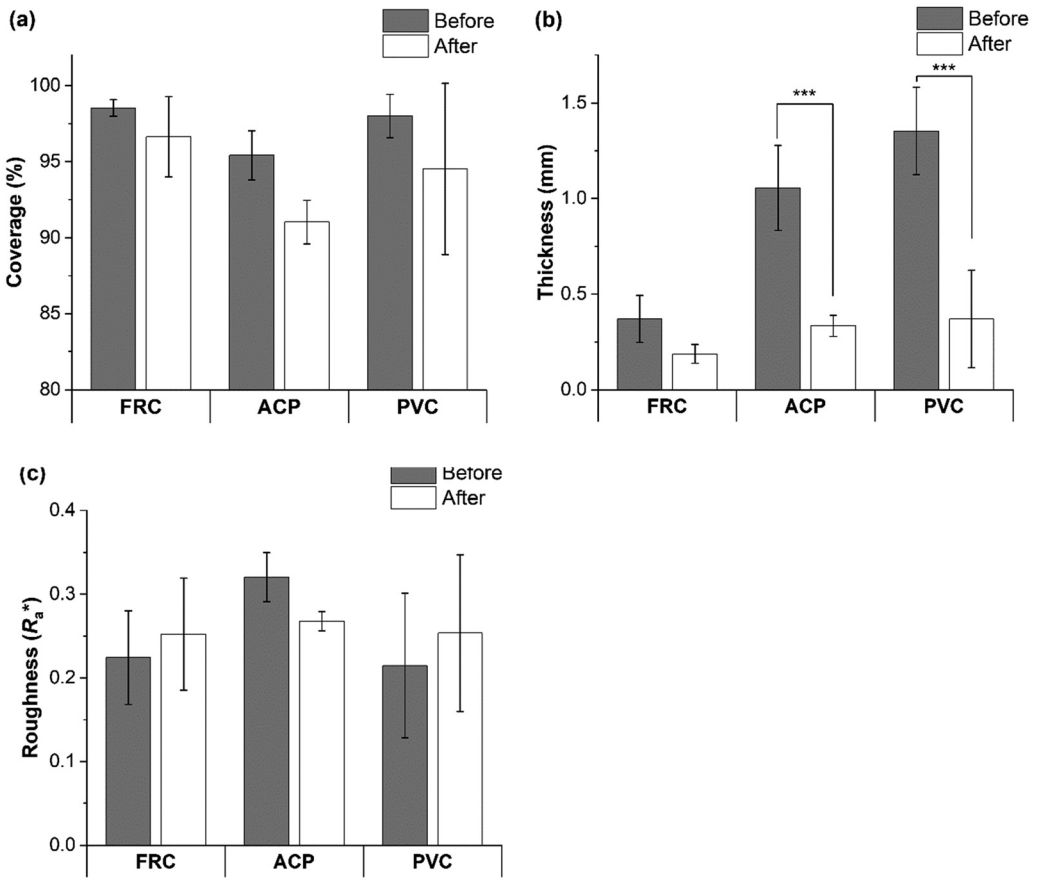

Fig. 4 Biofilm (a) coverage (%), (b) mean thickness (mm) and (c) roughness coefficient (R_a^*) calculated from OCT three-dimensional (3D) scans before and after rheological testing on a rheometer. Data is presented as mean ± SD. A '***' indicates a significant difference ($P < 0.001$) identified using a Welch's two sample T-test.

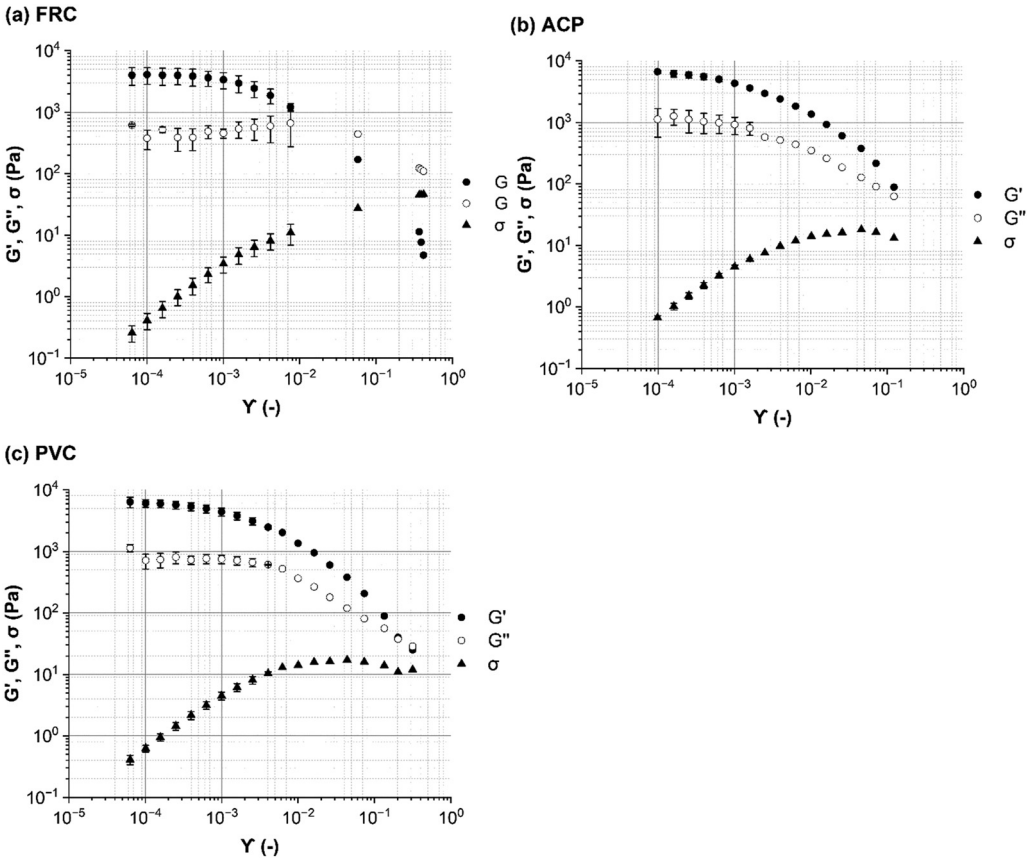

Fig. 5 Storage modulus (G', closed circles), loss modulus (G'', open circles) and stress (σ, closed triangles) *vs.* strain (γ) for biofilms grown on: (a) FRC (n = 2), (b) ACP (n = 2) and (c) PVC (n = 3) coupons. Data presented as mean ± SD.

maximum of G'',[53] as was found for the FRC biofilms (Fig. 5). After the G'' maximum the yield stress was reached and was followed by a slow decline in G'' with increasing strain. Unlike the other biofilms, the FRC biofilms also experienced an eight-fold increase in phase angle after the yield stress, which indicates a rapid shift from elastic-dominated to viscous-dominated behaviour.

3.2.2 Frequency sweeps. Fresh biofilm coupons were used to test the dynamic behaviour of marine biofilms over a range of frequencies, from 0.1 to 10 Hz or angular frequencies (ω) of 0.63 to 63 rad s^{-1}. G' was consistently higher than G'' for all coupons tested and both parameters were relatively independent of increasing frequency (Fig. 6). Collectively the behaviour displayed by the biofilms, across the conditions applied, is indicative of an elastic-solid material.

3.2.3 Creep-recovery. Effective shear modulus (G) and effective viscosity (η) were calculated from creep-recovery curves. The biofilms grown on FRC coupons possessed the lowest G and highest η when compared to the biofilms grown on ACP and PVC coupons (Fig. 7). All measurements were taken within the LVR region for each surface, as identified by the amplitude sweeps (Fig. 5 and Fig. S3, ESI†).

A shear stress of 1.5 Pa was identified as within the LVR region for all coupons tested (Fig. 5 and Fig. S3, ESI†) and was therefore used to compare the creep-recovery data (Fig. 8). The biofilms present on all coupon types showed similarity in the creep curves; each displayed an instantaneous elastic response (Fig. 8a), time-dependent viscous response (Fig. 8b) and instantaneous elastic recovery (Fig. S2, ESI†).

The suggestion that the FRC biofilms are the most compliant biofilms studied here is supported by the creep curves. Fig. 8 shows how the FRC biofilms deform more readily than the ACP and PVC biofilms with a greater instantaneous elasticity when strain was applied. Using the instantaneous elastic recovery portion which can be seen in Fig. S2 (ESI†), λ was calculated and revealed that FRC had the longest λ which was more than a factor of two greater than the alternative biofilms (Fig. 7).

It important to highlight that biofilms will display a different response under different stressors.[54] For example, within the LVR the FRC biofilms displayed stability and viscoelasticity, but at a higher shear stress structural integrity diminished. At 20 Pa the FRC biofilms flowed as a liquid and showed no viscoelastic strain recovery where the ACP biofilms maintained a time-dependant viscoelastic recovery response (Fig. S4, ESI†).

4. Discussion

To our knowledge, in this study ship-relevant marine biofilms have been rheologically characterised for the first time. The marine biofilms, grown at the Dove Laboratory, showed rheological

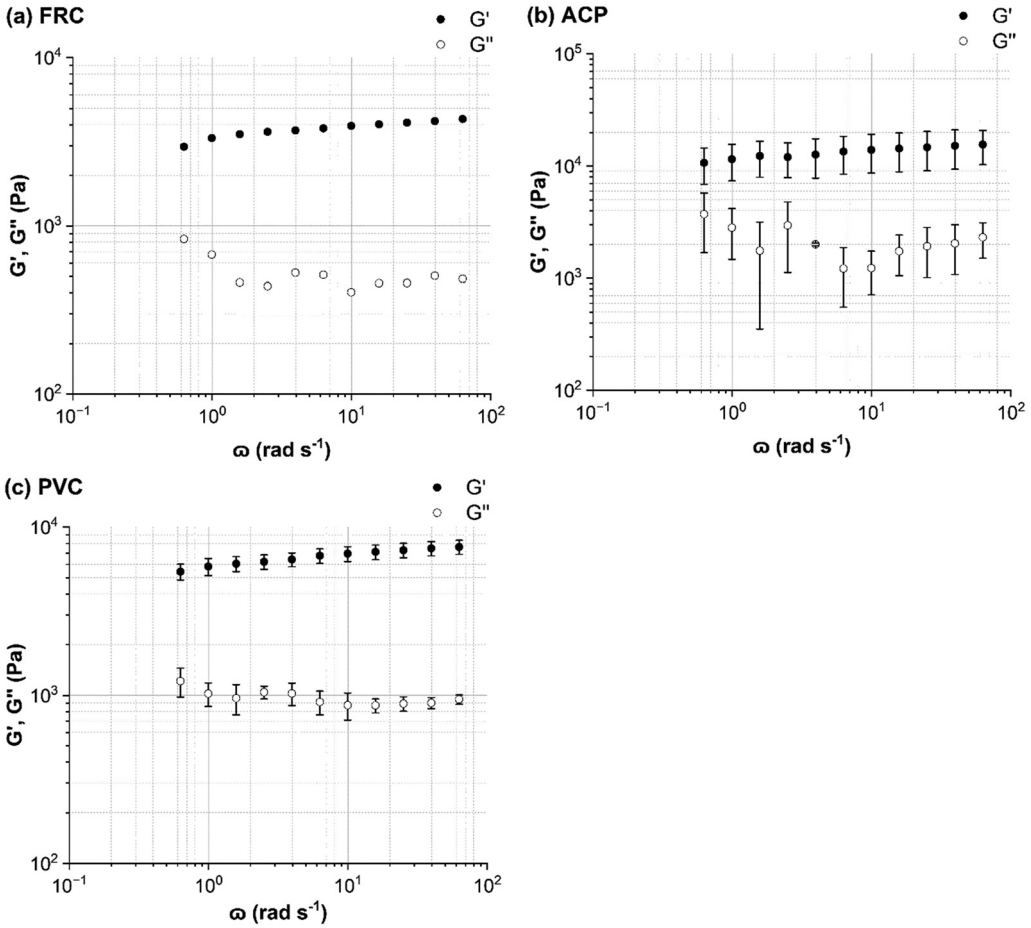

Fig. 6 Frequency sweeps performed on: (a) FRC (n = 1), (b) ACP (n = 2) and (c) PVC (n = 3). Angular frequency (ω) was incrementally increased from 0.63 to 63 rad s^{-1}. Storage modulus (G', closed circles) and loss modulus (G'', open circles) are plotted. Data presented as mean ± SD.

behaviour analogous to viscoelastic materials which has been reported previously for alternative biofilm types.[12,54–56] Some similarities were anticipated between the biofilms as they were grown under the same environmental conditions (temperature, pH, salinity, water depth) and the surface colour was kept consistent to avoid colour-driven changes to the biological communities. Despite some similarities, our observations show that there were significant differences, physically and mechanically, between biofilms grown on substantially chemically inert and biocide-free different surfaces. This was perhaps driven by differences in biological communities across the surfaces,[30] which would inevitably alter the physical structure and mechanical profile of a biofilm.

It is important to note that we aimed to assess the physico-mechanical properties of marine biofilms and therefore no taxonomic identification was executed. It would be of interest to carry out microbiological analysis of the biofilm components and community composition to determine whether differences observed in mechanical properties are caused by structural differences and/or biological ones.

4.1. Structural characterisation of marine biofilms using OCT

From optical microscopy and OCT cross-sectional scans (Fig. 3) it is shown how biofilms cultivated on different inert surfaces possess structural variability, thickness, and percent coverage.[44] The biofilms grown on ACP and PVC coupons could be described as thick and 'fluffy' (Fig. 4), where a 'fluffy' biofilm has loose surface layers and stiff consolidated base layers.[14,46,57–60] When a 'fluffy' biofilm is exposed to external stress the surface layers can be quickly sheared, whereas the base layers display a greater resistance.[57] Differences in OCT scans before and after testing on the rheometer showed that the ACP and PVC coupons displayed a 68% decline in biofilm thickness (Fig. 4) (Welch's two sample T-test, $P < 0.05$). Similar results were found for biofilms grown statically on an inert coating by Fabbri *et al.*,[44] where there was approximately a 70% decline in thickness after exposure to applied shear, coupled with a 40% reduction in coverage. In the present study, despite a significant reduction in thickness, percent coverage was comparable before and after rheological testing (Fig. 4) which suggests that the base layers of the biofilms were, in fact, more resistant to imposed shear than the surface layers. Interestingly, Zhang and Bishop noted that the base layers of a 'fluffy' biofilm can be 50% less porous than the surface layers which is important as a reduction in porosity leads to a less viscous, stiff, and dense biofilm.[57,61–63] Although, density and porosity were not investigated, it could be concluded that the ACP and

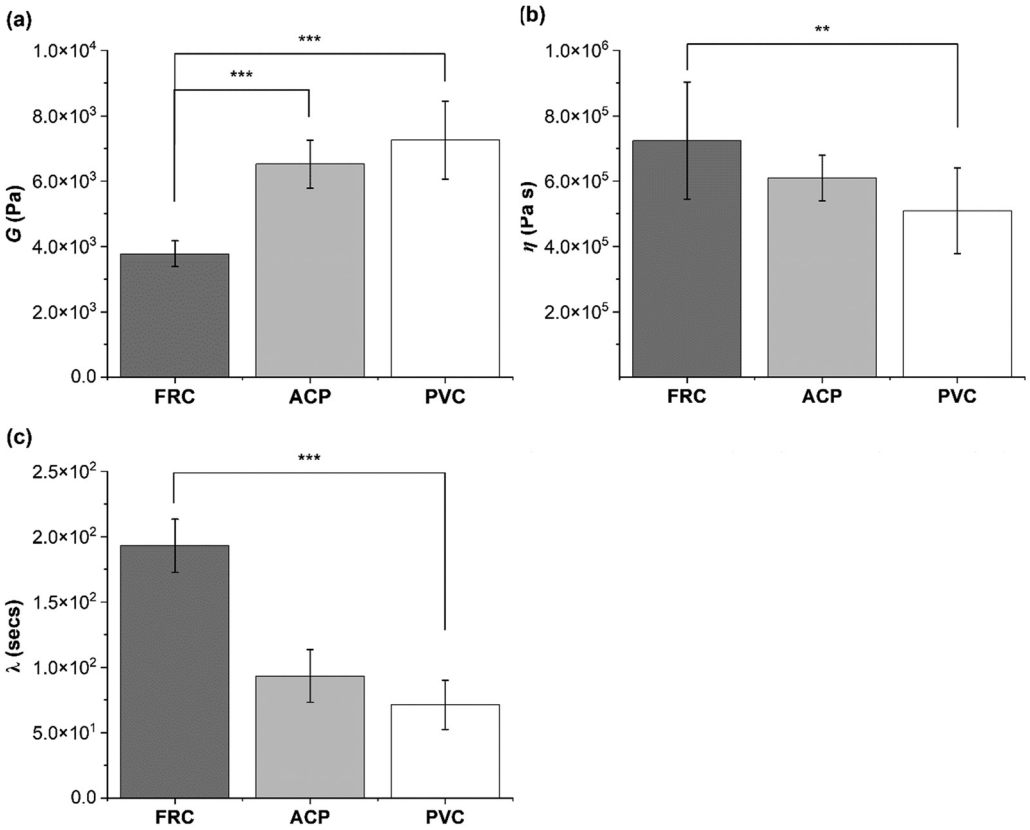

Fig. 7 Mechanical characterisation of marine biofilms grown on: FRC (n = 1), ACP (n = 1) and PVC (n = 3) coupons using creep-recovery measurements. (a) Shear modulus (G) was calculated using eqn (1); (b) viscosity (η) using eqn (2) and (c) elastic relaxation time (λ) using eqn (3). Statistical analysis was conducted using one-way ANOVA or Kruskal Wallis tests. Data presented as mean ± SD and P-values are represented as *** = 0.001, ** = 0.01.

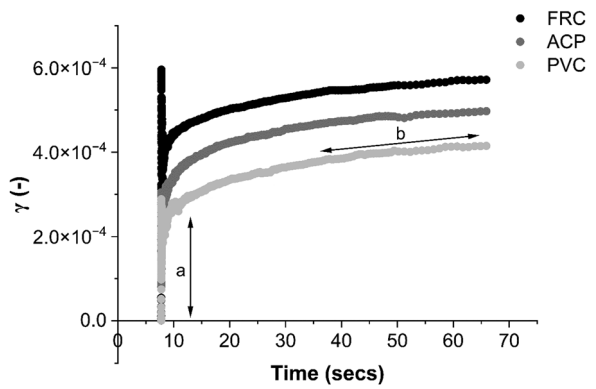

Fig. 8 Strain, γ (–) *vs.* time for each of the coupon types: FRC (black), ACP (dark grey) and PVC (light grey). A stress of 1.5 Pa was applied for 60 s at which point stress was set to 0 Pa and recovery was plotted for 60 s. The creep curve for PVC (light grey) has been annotated (black arrows) to show the two classic sections of a viscoelastic creep response: (a) instantaneous elastic response, (b) time-dependent viscous response.

PVC biofilms demonstrate characteristics akin with a 'fluffy' biofilm. The creep-recovery data further revealed that the ACP and PVC biofilms had a higher G, a lower η and shorter λ than the FRC biofilms (Fig. 7) which could be expected given the structural characteristics.

Alternatively, the biofilms grown on FRC coupons were much thinner than the ACP and FRC biofilms, measuring 0.37 ± 0.19 mm (Fig. 3 and 4b). Also, the FRC biofilms were sparse and displayed clumped coverage (Fig. 3). Like the ACP and PVC biofilms, the coverage of the FRC biofilms remained consistent before and after rheological testing; however, the FRC biofilms also showed no significant change in average biofilm thickness (Fig. 4). The FRC biofilms were not 'fluffy' like the other biofilms, and therefore it could be that differences in the physico-mechanical properties are driven by surface properties which are responsible for resistance of FRC biofilms. To confirm this, the rheological characterisation of marine biofilms on different coatings is required.

4.2. Viscoelasticity of marine biofilms

The effective G of marine biofilms ranged from 3780 to 7257 Pa, based on surface type, which fits comfortably within the range quoted in the open literature for other biofilms.[22–24] The biofilms grown on FRC coupons possessed a significantly lower G and higher η than the PVC and ACP biofilms (Fig. 7) and could be described as soft and viscous. Tierra *et al.*,[64] created a multicomponent model for studying biofilm deformation and determined that a biofilm with high viscosity and low elasticity is required for a stable and compliant biofilm structure.[64] A compliant biofilm can readily deform in response to imposed

shear stress due to viscoelastic behaviour; the elastic elements store energy *via* reversible deformation whereas viscous forces dissipate energy and reduce the risk of cohesive failure and detachment.[12,14] On the other hand, the ACP and PVC biofilms were stiff, possessed a lower yield stress and demonstrated significant removal of the biofilm surface layers. The reduction in thickness of the ACP and PVC biofilms could be responsible for the higher G exhibited due to consolidation effects.[65] From results presented, it can be concluded that the FRC biofilms were more compliant than the ACP and PVC biofilms as they adapted to changing conditions without removal (Fig. 4) and resisted imposed shear to a greater extent, as determined by the higher yield stress.

Souza-Egipsy[11] reported that an increase in G correlated with an increase in λ, due to a greater interconnectivity within the structure of biofilms collected from acidic environments. However, in the present study ACP and PVC biofilms possessed a significantly higher G but a λ more than half that for the FRC biofilms (Fig. 7). Peterson *et al.*,[8] found that a biofilm with a greater concentration of bacterial cells had a longer elastic relaxation time as cells are the heaviest component of the EPS, on the other hand, in the same study, it was noted that a longer λ could also be consequence to polymers re-arranging within the EPS. It is expected that polymeric structural rearrangement is responsible for the longer relaxation time exhibited by the softer FRC biofilms as an increased presence of bacterial cells within the EPS would produce a stiffer biofilm.[66,67]

The resistance of the FRC biofilms to applied stress was further highlighted in the amplitude sweeps where a weak strain overshoot was identified (Fig. 5a). A weak strain overshoot occurs during the yielding of a material and is a non-linear viscoelastic phenomenon caused by a shift from solid-like deformation in the LVR to fluid-like, plastic flow.[68] The FRC biofilms demonstrated viscoelastic solid behaviour at low stresses (Fig. 5a and 6a) and showed evidence of plasticity past the LVR (Fig. S3a, ESI†). A weak strain overshoot is characteristic of soft glassy materials such as emulsions, colloidal gels and soft hydrogel spheres dispersed in water[52,68] and has recently been observed in mono-species biofilms[37] and diatom-dominated biofilms found in an extreme acidic environment.[11] It is challenging to determine the structural cause of this behaviour as it material dependent,[52] and as biofilms are largely heterogeneous another level of complexity is added. It is likely that for the marine biofilms grown on FRC coupons the weak strain overshoot is caused by viscous dissipation and structural rearrangement as the biofilm adapts to increasing shear stress; as the critical stress is reached, the biofilm yields and alignment in the direction of flow occurs. This latter point fits with the phase-angle data that revealed an eight-fold decline after the yield stress was reached, which shows that the FRC biofilms were fluid-like past this point. Future work should incorporate the study of large amplitude oscillatory shear as although differences in mechanical response can be visualised from amplitude sweeps and creep-recovery, Lissajous plots provide a deeper insight into the mechanical state of a material during testing.[37,52]

4.3. Marine biofilm viscoelasticity and drag

Drag measurements were not studied here, however it could be expected that at low shear stress the FRC biofilms would produce a greater drag than the stiffer PVC and ACP biofilms due to greater compliance.[69] This is based on studies that have found compliant structures to generate a significantly higher drag compared to rigid alternatives,[20,70] particularly at lower shear.[69] Alternatively, rough and thick biofilms with good coverage are expected to provide a greater drag than thin and sparse biofilms,[20,71] which instead suggests that the PVC and ACP biofilms could produce a greater drag than the FRC biofilms. Valladares-Linares[65] determined that a decline in thickness was coupled with an increase in elasticity and consequently an increase in resistance to shear,[65] which could be explicable by denser base-layers that have consolidated over time under a thicker biofilm. On the other hand, Desmond *et al.*,[72] found no correlation between thickness, roughness and increased resistance to shear and Jafari *et al.*,[63] concluded that porosity influences resistance more than thickness. Collectively, these previous studies highlight the complexity of biofilms and how different growth, and testing conditions alter the physico-mechanical responses to imposed stress and making it challenging to link these properties to drag.

The ACP and PVC surfaces were chemically inert, they had no antifouling capabilities and the resultant biofilms shared similar structural and mechanical properties (Fig. 3–5 and 7). However, the FRC surfaces, which are also chemically inert but whose surface properties are designed to minimise adhesion of fouling organisms, appeared to select for patchy and compliant biofilms, and, for the most part, these had significantly different properties to the ACP and PVC biofilms. It is important to highlight that the experiments were executed at low shear stressors that are not comparable to those experienced on a ship or boat hull and therefore do not reflect in-service performance of different surfaces. Instead, the results highlight how different surfaces affect biofilm physico-mechanical properties and from the results presented it could be suggested that biofilm thickness plays a critical role in determining biofilm mechanics.[44]

Marine biofilms are likely affected by a multitude of environmental conditions, such as seasonality and temperature and testing conditions such as growth duration and surface type. Future work should endeavour to study how changing growth and testing conditions effects community structure and cascades down to altering biofilm viscoelasticity and inevitably drag. For example, biocidal coatings remain the most prevalent in the global shipping fleet when compared to the use of non-toxic coatings; as a result, it would be of interest to study how different coatings impact biofilm physico-mechanical properties. Similarly, longer-term experiments could be ran to capture seasonal variability. Although a parallel-plate rheometer may not mimic real-world conditions, with respect to the shear forces a biofilm could experience on a ship hull[73] it offers high throughput experiments for characterising marine biofilms on different surfaces and provides a benchmark for studying marine biofilm viscoelasticity. From characterising marine

biofilms under an array of different conditions and from working towards a standard method of testing, uncertainty analysis could be achieved which would enhance the findings from rheometer studies. Although uncertainty analysis could not be executed in the present study, we have started to answer questions on how marine biofilm structure interacts with mechanical properties and have suggested how this could implicate drag.

To date, it is unknown how surface coating and biofilm structure alter the mechanical response of biofilms to stress, but also how different biological communities influence these relationships. Before these questions can be answered, it is critical that the mechanical properties of marine biofilms are first studied in isolation to enable a better fundamental understanding of marine biofilm viscoelasticity and the role of biofilm structure in this behaviour.[8] This is an important step towards generating better informed coating formulation choices for improved fouling control properties and reduced drag.

5. Conclusion

To conclude ship-relevant marine biofilms, grown in natural seawater at the Dove Laboratory (Cullercoats Bay, UK) are viscoelastic and their physico-mechanical properties differ depending on the surface type. To our knowledge, we provide the first viscoelastic characterization of different marine biofilms using creep-recovery experiments on a parallel-plate rheometer. The viscoelastic biofilms grown on ACP and PVC coupons displayed similarities in their structural properties and in their mechanical response to imposed shear as shown by the amplitude sweeps (Fig. 5). The FRC biofilms, however, had a higher yield stress, significantly lower G, higher η, and a λ more than double that of the alternative biofilms. Collectively, the FRC biofilms could be described as soft and viscous and were more compliant than the ACP and PVC biofilms. Structurally, the ACP and PVC biofilms could be described as 'fluffy' and thick, whereas the FRC biofilms were thinner and did not show a significant decline in thickness before and after rheological testing. It would be beneficial to determine a correlation between biofilm physico-mechanical properties and biofilm composition as a function of coating type, as it is likely that differences observed across the biofilms grown on different coupons are partly explicable by microbiological differences. We acknowledge that there are additional properties that could have altered the biofilm physico-mechanics that have not been studied here, such as the wettability and chemical composition of the coatings, as well as biofilm community. Nevertheless, we have highlighted how different surface treatments produce biofilms with different physico-mechanical properties which is an important research area for the shipping and coatings industry.

Author contribution

Alexandra Snowdon: conceptualization, methodology, validation, formal analysis, investigation, resources, writing – original draft, writing – review & editing, visualization. Simon Dennington: methodology, writing – original draft, writing – review & editing. Jennifer Longyear: conceptualization, methodology, resources, writing – original draft, writing – review & editing, supervision, funding acquisition. Julian Wharton: conceptualization, methodology, writing – original draft, writing – review & editing, supervision, funding acquisition. Paul Stoodley: conceptualization, methodology, writing – original draft, writing – review & editing, funding acquisition.

Conflicts of interest

The work was sponsored, in part, by AkzoNobel through Paul Stoodley. Employees of AkzoNobel were involved in the work (Jennifer Longyear).

Acknowledgements

This work was funded by a DTP ESPRC grant EP/R513325/1 to the University of Southampton and AkzoNobel. The authors would like to thank Dr Alistair Finnie for editorial review.

References

1 K. A. Zargiel, J. S. Coogan and G. W. Swain, Diatom community structure on commercially available ship hull coatings, *Biofouling*, 2011, **27**(9), 955–965. Available from: **https://www.tandfonline.com/action/journalInformation?journalCode=gbif20**.

2 K. A. Zargiel and G. W. Swain, Static vs dynamic settlement and adhesion of diatoms to ship hull coatings, *Biofouling*, 2014, **30**(1), 115–129. Available from: **http://www.tandfonline.com/doi/abs/10.1080/08927014.2013.847927**.

3 M. G. Mazza, The physics of biofilms—an introduction, *J. Phys. D: Appl. Phys.*, 2016, **49**(20), 203001. Available from: **https://iopscience.iop.org/article/10.1088/0022-3727/49/20/203001**.

4 J. N. Wilking, T. E. Angelini, A. Seminara, M. P. Brenner and D. A. Weitz, Biofilms as Complex Fluids, *Mater. Res. Soc. Bull.*, 2011, **36**, 385–390. Available from: **www.mrs.org/bulletin**.

5 G. M. Kavanagh and S. B. Ross-Murphy, Rheological characterisation of polymer gels, in *Progress in Polymer Science*, Elsevier Ltd, 1998, vol. 23, pp. 533–562.

6 P. Lembre, C. Lorentz and P. Di, Exopolysaccharides of the Biofilm Matrix: A Complex Biophysical World, in *The Complex World of Polysaccharides*, InTech, 2012.

7 S. G. V. Charlton, M. A. White, S. Jana, L. E. Eland, P. G. Jayathilake and J. G. Burgess, *et al.*, Regulating, Measuring, and Modeling the Viscoelasticity of Bacterial Biofilms, *J. Bacteriol.*, 2019, **201**(18), e00101–19.

8 B. W. Peterson, Y. He, Y. Ren, A. Zerdoum, M. R. Libera and P. K. Sharma, *et al.*, Viscoelasticity of biofilms and their recalcitrance to mechanical and chemical challenges, in

FEMS Microbiology Reviews, Oxford University Press, 2015, vol. 39, pp. 234–245.

9 A. M. Grillet, N. B. Wyatt and L. M. Gloe, Polymer Gel Rheology and Adhesion, *Rheology*, 2012, 59–78; Available from: **https://www.intechopen.com/chapters/30968**.

10 T. L. Sun, T. Kurokawa, S. Kuroda, I. A. Bin, T. Akasaki and K. Sato, *et al.*, Physical hydrogels composed of polyampholytes demonstrate high toughness and viscoelasticity, *Nat. Mater.*, 2013, **12**(10), 932–937.

11 V. Souza-Egipsy, J. F. Vega, E. González-Toril and Á. Aguilera, Biofilm mechanics in an extremely acidic environment: microbiological significance, *Soft Matter*, 2021, **17**(13), 3672. Available from: **https://pubs.rsc.org/en/content/articlehtml/2021/sm/d0sm01975e**.

12 C. J. Rupp, C. A. Fux and P. Stoodley, Viscoelasticity of Staphylococcus aureus biofilms in response to fluid shear allows resistance to detachment and facilitates rolling migration, *Appl. Environ. Microbiol.*, 2005, **71**(4), 2175–2178.

13 P. Stoodley, J. D. Boyle and H. M. Lappin-scott, Influence of flow on the structure of bacterial biofilms, in *Microbial Biosystems: New Frontiers, Proceedings of the 8th International Symposium on Microbial Ecology*, ed. Bell C. R., Brylinsky M. and Johnson-Green P. C., 2000. pp. 263–269. Available from: **https://eprints.soton.ac.uk/id/eprint/157631**.

14 E. S. Gloag, D. J. Wozniak, P. Stoodley and L. Hall-Stoodley, Mycobacterium abscessus biofilms have viscoelastic properties which may contribute to their recalcitrance in chronic pulmonary infections, *Sci. Rep.*, 2021, **11**, 5020, DOI: **10.1038/s41598-021-84525-x**.

15 R. L. Townsin, The Ship Hull Fouling Penalty, *Biofouling*, 2003, **19**, 9–15. Available from: **https://www.tandfonline.com/action/journalInformation?journalCode=gbif20**.

16 E. G. Haslbeck and G. S. Bohlander, Microbial Biofilm Effects on Drag. Ship Production Symposium, 1992.

17 M. P. Schultz, J. A. Bendick, E. R. Holm and W. M. Hertel, Economic impact of biofouling on a naval surface ship, *Biofouling*, 2011, **27**(1), 87–98. Available from: **https://www.tandfonline.com/doi/full/10.1080/08927014.2010.542809**.

18 J. M. Andrewartha and J. E. Sargison Turbulence and Mean-Velocity Structure of Flows over Filamentous Biofilms, In: Proceedings of the 24th IAHR World Congress, 2011 [cited 2020 Sep 23]. Available from: **http://ecite.utas.edu.au/76555**.

19 L. F. Moody, Friction factors for pipe flow, *Trans. ASME*, 1944, **66**, 671–684. Available from: **http://www.ipt.ntnu.no/~asheim/TPG4135/Moody.pdf**.

20 J. D. Hartenberger, E. G. Callison, J. W. Gose, M. Perlin and S. L. Ceccio, Drag production mechanisms of filamentous biofilms, *Biofouling*, 2020, 736–752; Available from: **https://www.tandfonline.com/action/journalInformation?journalCode=gbif20**.

21 P. Stoodley, Z. Lewandowski, J. D. Boyle and H. M. Lappin-Scott, Oscillation characteristics of biofilm streamers in turbulent flowing water as related to drag and pressure drop, *Biotechnol. Bioeng.*, 1998, **57**(5), 536–544.

22 Y. M. Kim, T. H. Kwon and S. Kim, Measuring elastic modulus of bacterial biofilms in a liquid phase using atomic force microscopy, *Geomech. Eng.*, 2017, **12**(5), 863–870.

23 M. Tallawi, M. Opitz and O. Lieleg, Modulation of the mechanical properties of bacterial biofilms in response to environmental challenges, in *Biomaterials Science*, Royal Society of Chemistry, 2017, vol. 5, pp. 887–900.

24 M. Böl, A. E. Ehret, A. B. Albero, J. Hellriegel and R. Krull, Recent advances in mechanical characterisation of biofilm and their significance for material modelling, *Crit. Rev. Biotechnol.*, 2013, **33**(2), 145–171. Available from: **https://www.tandfonline.com/action/journalInformation?journalCode=ibty20**.

25 M. Winston, C. J. Rupp, A. M. Vinogradov, B. W. Towler, H. Adams and P. Stoodley, Rheology of Biofilms, *Proc ASCE 16th Eng. Mech. Conf.*, 2003, 1–5. Available from: **www.ce.washington.edu/em03/proceedings/papers/548.pdf**.

26 A. A. Finnie and D. N. Williams, Paint and Coatings Technology for the Control of Marine Fouling, *Biofouling*, 2010, 185–206.

27 B. Galvão De Campos, J. Figueiredo, F. Perina, D. Moledo De Souza Abessa, S. Loureiro and R. Martins, *et al.*, Occurrence, effects and environmental risk of antifouling biocides (EU PT21): are marine ecosystems threatened?, *Crit. Rev. Environ. Sci. Technol.*, 2022, **52**(18), 3179–3210. Available from: **https://www.tandfonline.com/action/journalInformation?journalCode=best20**.

28 M. Atlar, C. Anderson, M. Callow, M. Candries, A. Milne and R. L. Townsin, The development of foul-release coatings for seagoing vessels, *J. Mar. Des. Oper.*, 2003, (B4), 11–23. Available from: **https://www.researchgate.net/publication/238575879**.

29 M. Candries, M. Atlar and C. D. Anderson, Estimating the impact of new-generation antifoulings on ship performance: the presence of slime, *J. Mar. Eng. Technol.*, 2003, **2**(1), 13–22. Available from: **https://www.tandfonline.com/action/journalInformation?journalCode=tmar20**.

30 M. Papadatou, S. C. Robson, S. Dobretsov, J. E. M. Watts, J. Longyear and M. Salta, Marine biofilms on different fouling control coating types reveal differences in microbial community composition and abundance, *MicrobiologyOpen*, 2021, **10**(4), e1231.

31 M. Salta, J. A. Wharton, Y. Blache, K. R. Stokes and J. F. Briand, Marine biofilms on artificial surfaces: structure and dynamics, *Environ. Microbiol.*, 2013, **15**, 2879–2893.

32 J. Schiebel, J. Noack, S. Rödiger, A. Kammel, F. Menzel and K. Schwibbert, *et al.*, Analysis of three-dimensional biofilms on different material surfaces, *Biomater. Sci.*, 2020, **8**, 3500.

33 R. M. Donlan, Biofilms: Microbial Life on Surfaces, *Emerging Infect. Dis.*, 2002, **8**, 881–888. Available from: **http://www.microbelibrary.org/**.

34 K. Z. Hunsucker, G. J. Vora, J. T. Hunsucker, H. Gardner, D. H. Leary and S. Kim, *et al.*, Biofilm community structure and the associated drag penalties of a groomed fouling release ship hull coating, *Biofouling*, 2018, **34**(2), 162–172. Available from: **https://www.tandfonline.com/doi/abs/10.1080/08927014.2017.1417395**.

35 V. D. Gordon, M. Davis-Fields, K. Kovach and C. A. Rodesney, Biofilms and mechanics: a review of experimental techniques and findings, *J. Phys. D: Appl. Phys.*, 2017, **50**, 223003.
36 E. S. Gloag, S. Fabbri, D. J. Wozniak and P. Stoodley, Biofilm mechanics: implications in infection and survival, *Biofilm*, 2020, **2**, 100017.
37 S. Jana, S. G. V. Charlton, L. E. Eland, J. G. Burgess, A. Wipat and T. P. Curtis, *et al.*, Nonlinear rheological characteristics of single species bacterial biofilms, *npj Biofilms Microbiomes*, 2020, **6**(1), 19.
38 H. Boudarel, J. D. Mathias, B. Blaysat and M. Grédiac, Towards standardized mechanical characterization of microbial biofilms: analysis and critical review, *npj Biofilms Microbiomes*, 2018, **4**, 17.
39 M. Gambino, P. Sanmartín, M. Longoni, F. Villa, R. Mitchell and F. Cappitelli, Surface colour: an overlooked aspect in the study of cyanobacterial biofilm formation, *Sci. Total Environ.*, 2019, **659**, 342–353.
40 S. Dobretsov, R. M. M. Abed and C. R. Voolstra, The effect of surface colour on the formation of marine micro and macrofouling communities, *Biofouling*, 2013, **29**(6), 617–627. Available from: **https://www.tandfonline.com/action/journalInformation?journalCode=gbif20**.
41 I. C. Davidson, G. Smith, G. V. Ashton, G. M. Ruiz and C. Scianni, An experimental test of stationary lay-up periods and simulated transit on biofouling accumulation and transfer on ships, *Biofouling*, 2020, **36**(4), 455–466. Available from: **https://www.tandfonline.com/doi/abs/10.1080/08927014.2020.1769612**.
42 M. Wagner and H. Horn, Optical coherence tomography in biofilm research: a comprehensive review, *Biotechnol. Bioeng.*, 2017, **114**(7), 1386–1402.
43 *MATLAB. 9.11.0.1837725 (R2021b)*, The Maths Works Inc., Natick, Massachusetts, 2021.
44 S. Fabbri, S. P. Dennington, C. Price, P. Stoodley and J. Longyear, A marine biofilm flow cell for in situ screening marine fouling control coatings using optical coherence tomography, *Ocean Eng*, 2018, **170**, 321–328.
45 F. Blauert, H. Horn and M. Wagner, Time-resolved biofilm deformation measurements using optical coherence tomography, *Biotechnol. Bioeng.*, 2015, **112**(9), 1893–1905.
46 B. W. Towler, C. J. Rupp, A. L. B. Cunningham and P. Stoodley, Viscoelastic Properties of a Mixed Culture Biofilm from Rheometer Creep Analysis, *Biofouling*, 2003, **19**(5), 279–285.
47 E. S. Gloag, G. K. German, P. Stoodley and D. J. Wozniak, Viscoelastic properties of Pseudomonas aeruginosa variant biofilms, *Sci. Rep.*, 2018, **8**(1), 1–11, DOI: **10.1038/s41598-018-28009-5**.
48 T. Shaw, M. Winston, C. J. Rupp, I. Klapper and P. Stoodley, Commonality of elastic relaxation times in biofilms, *Phys. Rev. Lett.*, 2004, **93**(9), 1–4.
49 R Core team, *R: A language and environment for statistical computing, R Foundation for Statistical Computing*. 2020.
50 A. M. Vinogradov, M. Winston, C. J. Rupp and P. Stoodley, Rheology of biofilms formed from the dental plaque pathogen Streptococcus mutans, *Biofilms*, 2004, **1**(1), 49–56.
51 L. Prades, S. Fabbri, A. D. Dorado, X. Gamisans, P. Stoodley and C. Picioreanu, Computational and experimental investigation of biofilm disruption dynamics induced by high velocity gas jet impingement, *Am. Soc. Microbiol.*, 2020, **11**(1), e02813–e02819.
52 K. Hyun, M. Wilhelm, C. O. Klein, K. Soo Cho, J. Gun Nam and K. Hyun Ahn, *et al.*, A review of nonlinear oscillatory shear tests: analysis and application of large amplitude oscillatory shear (LAOS), *Prog. Polym. Sci.*, 2011, **36**, 1697–1753.
53 K. Hyun and W. Kim, A new non-linear parameter Q from FT-Rheology under nonlinear dynamic oscillatory shear for polymer melts system, *Korea Aust. Rheol. J.*, 2011, **23**(4), 227–235.
54 P. Stoodley, Z. Lewandowski, J. D. Boyle and H. M. Lappin-Scott, Structural deformation of bacterial biofilms caused by short-term fluctuations in fluid shear: an in situ investigation of biofilm rheology, *Biotechnol. Bioeng.*, 1999, **65**(1), 83–92.
55 V. Vadillo-Rodriguez and J. R. Dutcher, Dynamic viscoelastic behavior of individual Gram-negative bacterial cells, *Soft Matter*, 2009, **5**, 5012–5019. Available from: **www.rsc.org/softmatter**.
56 V. Körstgens, H. C. Flemming, J. Wingender and W. Borchard, Uniaxial compression measurement device for investigation of the mechanical stability of biofilms, *J. Microbiol. Methods*, 2001, **46**(1), 9–17.
57 T. C. Zhang and P. L. Bishop, Density, porosity, and pore structure of biofilms, *Water Res.*, 1994, **28**(11), 2267–2277.
58 E. Paramonova, O. J. Kalmykowa, H. C. Van Der Mei, H. J. Busscher and P. K. Sharma, Impact of hydrodynamics on oral biofilm strength, *J. Dent. Res.*, 2009, **88**(10), 922–926.
59 C. S. Laspidou and N. Aravas, Variation in the mechanical properties of a porous multi-phase biofilm under compression due to void closure, *Water Sci. Technol.*, 2007, **55**(8), 447–453.
60 C. Picioreanu, F. Blauert, H. Horn and M. Wagner, Determination of mechanical properties of biofilms by modelling the deformation measured using optical coherence tomography, *Water Res.*, 2018, **145**, 588–598, DOI: **10.1016/j.watres.2018.08.070**.
61 P. Lembré, P. Di Martino and C. Vendrely, Amyloid peptides derived from CsgA and FapC modify the viscoelastic properties of biofilm model matrices, *Biofouling*, 2014, **30**(4), 415–426. Available from: **http://www.tandfonline.com/doi/abs/10.1080/08927014.2014.880112**.
62 C. S. Laspidou, L. A. Spyrou, N. Aravas and B. E. Rittmann, Material modeling of biofilm mechanical properties, *Math. Biosci.*, 2014, **251**(1), 11–15.
63 M. Jafari, P. Desmond, M. C. M. van Loosdrecht, N. Derlon, E. Morgenroth and C. Picioreanu, Effect of biofilm structural deformation on hydraulic resistance during ultrafiltration: a numerical and experimental study, *Water Res.*, 2018, **145**, 375–387.
64 G. Tierra, J. P. Pavissich, R. Nerenberg, Z. Xu and M. S. Alber, Multicomponent model of deformation and detachment

of a biofilm under fluid flow, *J. R. Soc., Interface*, 2015, **12**(106), 20150045. Available from: **https://royalsocietypublishing.org/doi/10.1098/rsif.2015.0045**.

65 R. Valladares Linares, A. D. Wexler, S. S. Bucs, C. Dreszer, A. Zwijnenburg and H. C. Flemming, *et al.*, Compaction and relaxation of biofilms, *Desalin Water Treat.*, 2016, **57**(28), 12902–12914.

66 H. Cao, O. Habimana, A. Safari, R. Heffernan, Y. Dai and E. Casey, Revealing region-specific biofilm viscoelastic properties by means of a micro-rheological approach, *npj Biofilms Microbiomes*, 2016, **2**(1), 1–7.

67 P. Barai, A. Kumar and P. P. Mukherjee, Modeling of mesoscale variability in biofilm shear behavior, *PLoS One*, 2016, **11**(11), e0165593.

68 G. J. Donley, P. K. Singh, A. Shetty, S. A. Rogers and D. A. Weitz, Elucidating the G'' overshoot in soft materials with a yield transition via a time-resolved experimental strain decomposition, *Proc. Natl. Acad. Sci. U. S. A.*, 2020, **117**(36), 21945–21952. Available from: **www.pnas.org/cgi/doi/10.1073/pnas.2003869117**.

69 A. Snowdon, S. Q. An, A. Finnie, M. Dale, S. Dennington and J. Longyear, *et al.*, Elastomeric sandpaper replicas as model systems for investigating elasticity, roughness and associated drag in a marine biofilm flow cell, *Ocean Eng.*, 2022, **266**, 112739.

70 B. F. Picologlou, N. Zelver and W. G. Characklis, Biofilm growth and hydraulic performance, *J. Hydraul Div.*, 1980, **106**(HY5), 733–746.

71 E. A. K. Murphy, J. M. Barros, M. P. Schultz, K. A. Flack, C. N. Steppe and M. A. Reidenbach, Boundary layer hydrodynamics of patchy biofilms, *Biofouling*, 2022, **37**(7), 696–714. Available from: **https://www.tandfonline.com/action/journalInformation?journalCode=gbif20**.

72 P. Desmond, E. Morgenroth and N. Derlon, Physical structure determines compression of membrane biofilms during Gravity Driven Membrane (GDM) ultrafiltration, *Water Res.*, 2018, **143**, 539–549.

73 A. Karimi, D. Karig, A. Kumar and A. M. Ardekani, Interplay of Physical Mechansism and Biofilm Processes: Review of Microfluidic Methods, *Lab Chip.*, 2015, **15**(1), 23–42.